

Current Biology, Volume 28

Supplemental Information

Multifunctional Wing Motor Control of Song and Flight

Angela O'Sullivan, Theodore Lindsay, Anna Prudnikova, Balazs Erdi, Michael Dickinson, and Anne C. von Philipsborn

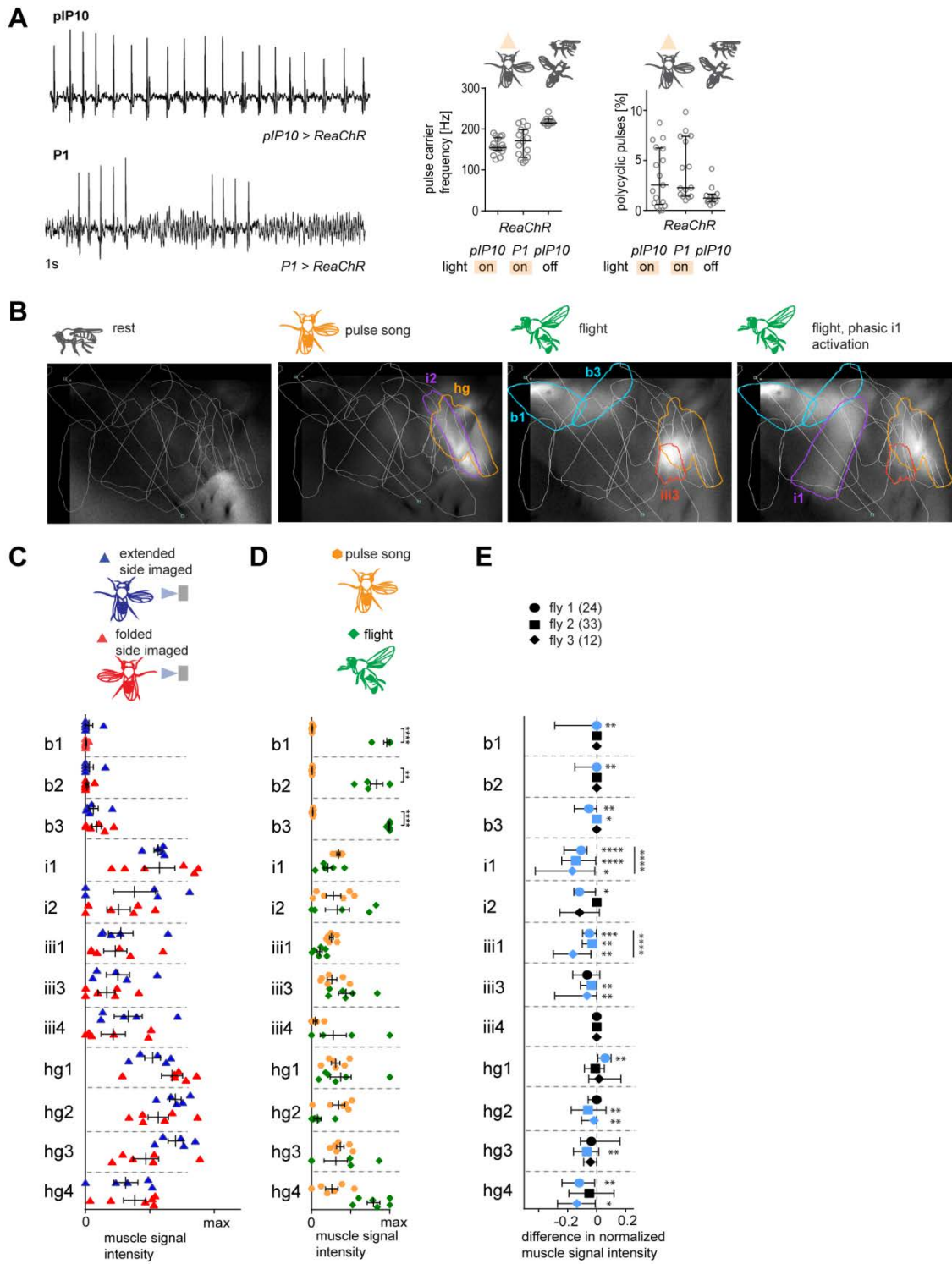


Figure S1. GCaMP imaging of ontogenetically triggered song. Related to Figure 2.

A Example oscillograms (1s) of song triggered by optogenetic activation of pIP10 (*pIP10 > ReaChR*) and P1 (*P1 > ReaChR*) of tethered flies expressing GCaMP in steering muscles. Song is close to natural, but pulse frequency is slightly decreased and percentage of polycyclic pulses slightly increased compared to song of untethered *pIP10 > ReaChR* males singing to a female. **B** Example of raw images of GCaMP fluorescence (from a *pIP10 > ReaChR* fly) with location of muscles outlined. During pulse song, b muscles are silent and hg and i2 muscles light up. In contrast, during flight, b1 and b3 and iii3 are tonically active. Fluorescence in the hg group is dominated by hg4. Occasionally, phasic i1 activation can be observed. b1 and b3 are outlined in cyan, i1 and i2 in purple, iii3 in red and hg1-4 in orange. See also video S1. **C** Normalized mean GCaMP signals during song bouts at the side of the extended (in blue) and folded (in red) wing. Each data point represents one fly (n=7), black bars are mean with SEM. There is no significant difference between signals during song bouts song from the two different wings (Kruskal-Wallis test with Dunn's multiple comparison of the full data set and Friedman test with Dunn's multiple comparison for paired data from flies which sang with both wings). Data from pIP10 triggered pulse song (*pIP10 > ReaChR*). **D** Normalized mean GCaMP signals during song bouts (in orange) and sustained flight (in green), data from P1 triggered pulse episodes (*P1 > ReaChR*). Each data point represents one fly (n=5), black bars are mean with SEM. **p<0.01, ****p<0.0001 (ANOVA, Holm-Sidak's multiple comparison correction). Compared to data from pIP10 triggered song, hg muscles are less active. For details about differences between pIP10 and P1 evoked singing, see STAR methods. **E** Changes in normalized mean GCaMP signals when flies switch from pulse to sine song episodes (data from 3 flies with n=24, 33 and 12 sine episodes). Blue data points indicate significance (Wilcoxon matched-pairs test). For i1 and iii1, muscles signal significantly decreased in all flies (****p<0.0001, Wilcoxon matched-pairs test on pooled data of n=69 sine episodes) compared to the 250 ms preceding pulse song. Data from P1 triggered song (*P1 > ReaChR*). For full genotypes of experimental flies, see Table S2.

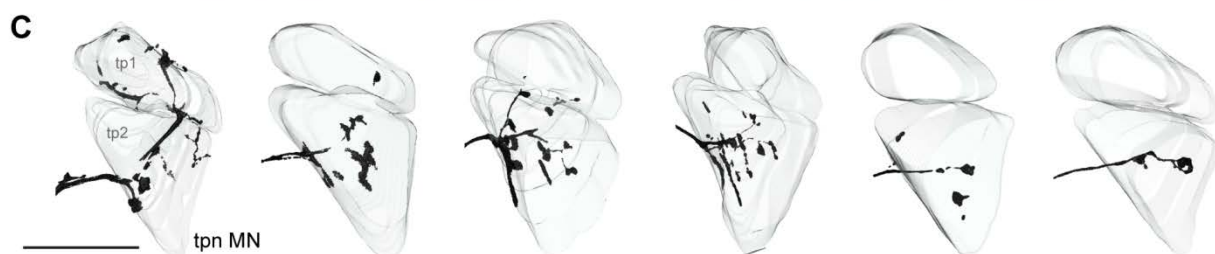
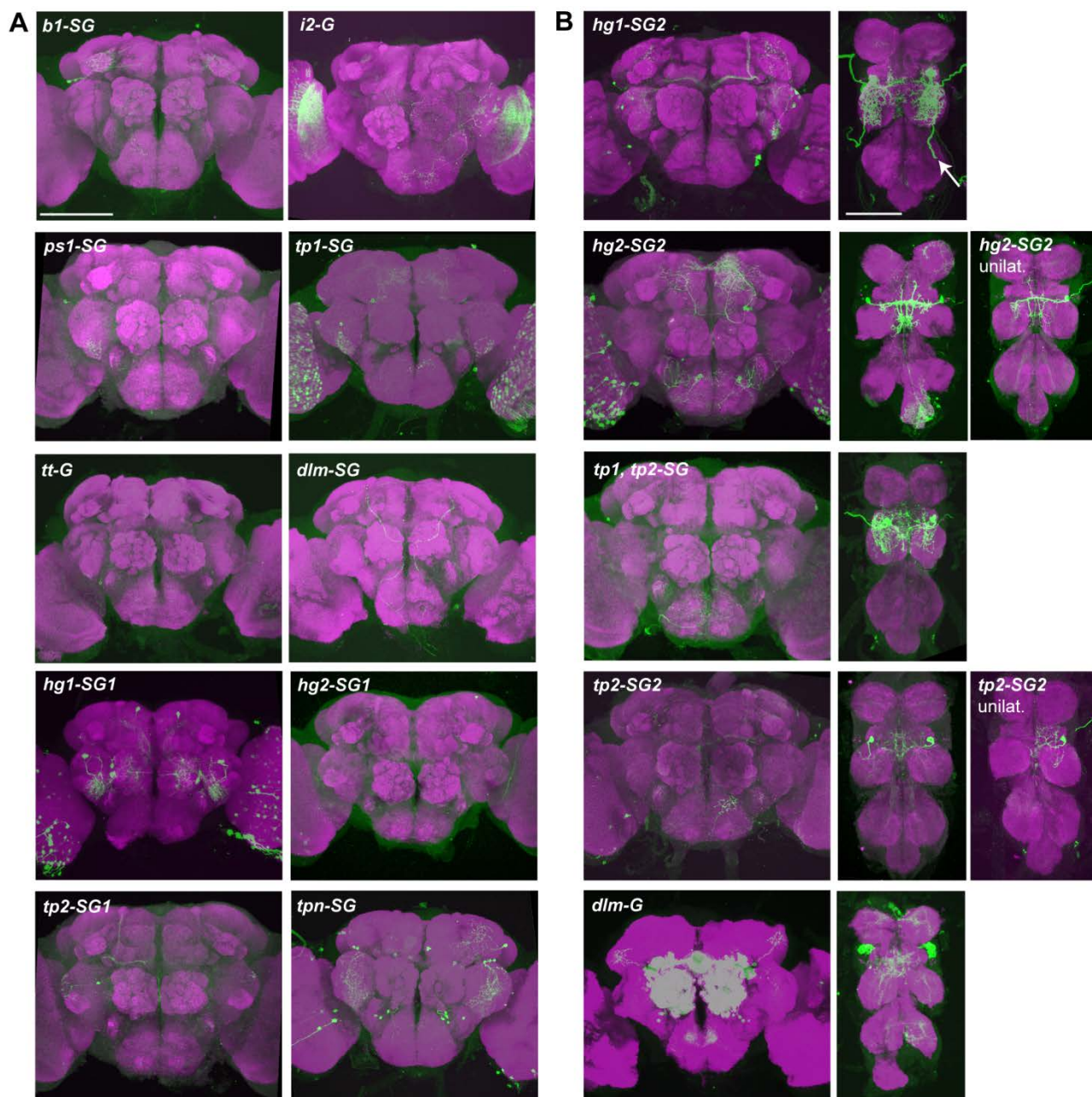


Figure S2. Expression patterns of motor neuron driver lines. Related to Figure 3.

A Brain expression patterns of main driver lines for wing MNs shown in Figure 3A (GFP expression in green, neuropil anti-bruchpilot staining in magenta). **B** Expression patterns of additional driver lines for *hg1*, *hg2*, *tp2*, *tp1+tp2* and *dln* MNs. *hg1-SG2* labels a second MN (axon marker with white arrow) which does not innervate wing muscles. Unilateral expression in *tp2* and *hg2* MN is occasionally observed for *tp2-SG2* and *hg2-SG1*. **C** Representative examples of muscle innervation patterns of *tpn* MN. Scale bars: 100 μ m. For full genotypes of experimental flies, see Table S2.

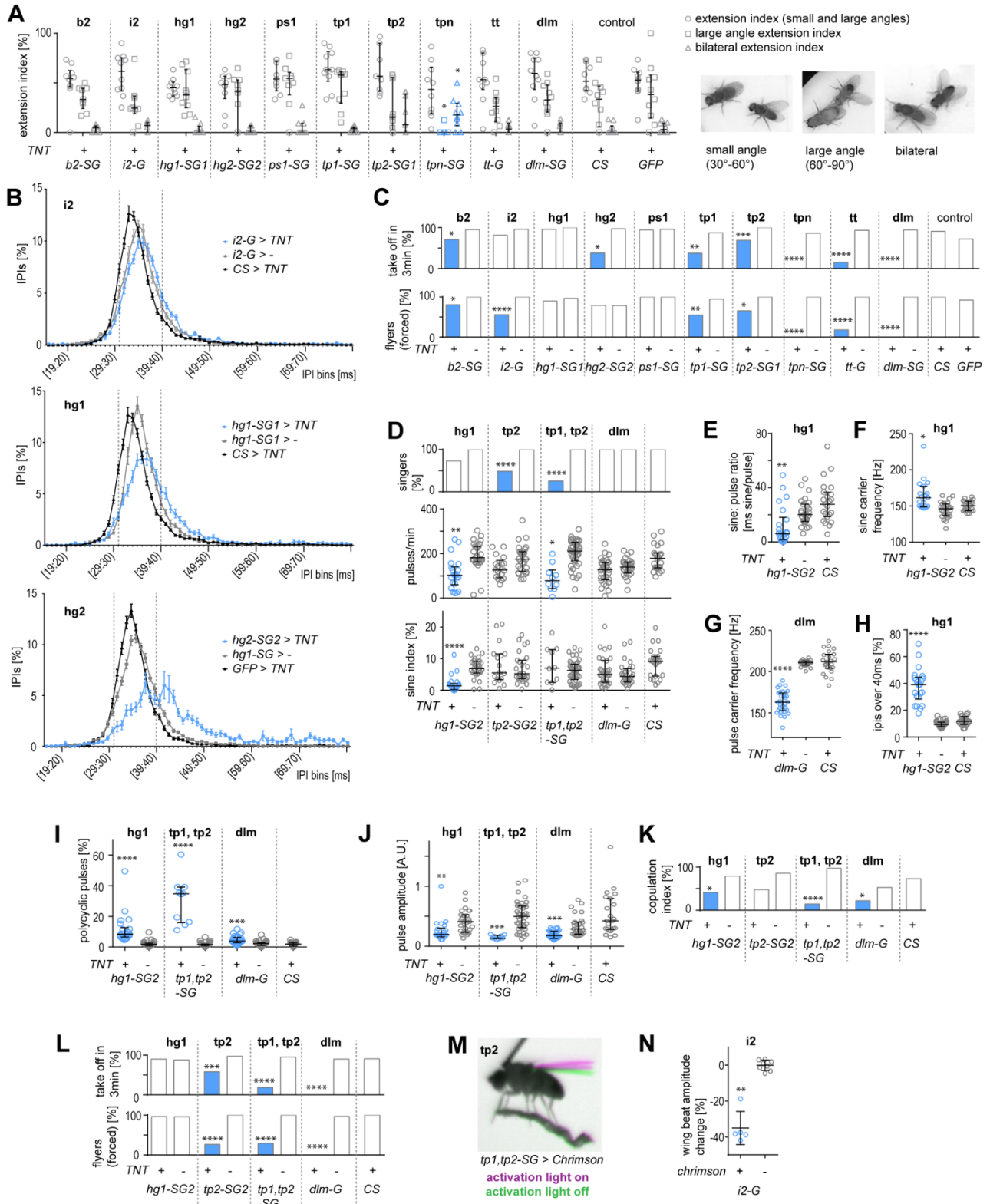


Figure S3. Wing motor neurons affect song and flight ability. Related to Figure 4.

A Wing extension patterns upon silencing of wing MNs. The extension index is the fraction of evaluated video frames for which a fly extended a wing, the large angle index the fraction of wing extensions with an angle larger than 60° (of all extensions), and the bilateral extension index the fraction of wing extension with two wings extended for at least 30° (of all extensions). Examples of wing extension categories are shown to the right. **B** Inter pulse interval distributions upon silencing of i2, hg1 and hg2 MN, showing fewer ipis in the range of 30-40 ms and an increased number of ipis longer than 40 ms. For each 1 ms bin, the mean percentage of ipis is plotted, error bars show standard errors. N= 20-30 flies per genotype. **C** Flight ability upon silencing of wing MNs. Proportion of flies being able to take off and fly for a distance of at least 15cm (upper graph) and flight ability in a forced flight drop assay (lower graph). **D** Courtship song production of male flies with wing MNs silenced by expression of tetanus toxin (*TNT*), data from additional, independent genetic driver lines for hg1, tp2, tp1+tp2 and dlm MNs. **E** Specific reduction of sine song compared to pulse song upon silencing of hg1 MN with a second driver line, *hg1-SG2*. **F** Increased sine song carrier frequency upon silencing of hg1 MN with *hg1-SG2*. **G** Decrease in pulse carrier frequency upon silencing of dlm MNs with a second driver line, *dlm-G*. **H** Inter pulse interval (ipi) distributions shift upon silencing of hg1 MN with *hg1-SG2*. **I** Increased occurrence of polycyclic pulses upon silencing of hg1, tp1+tp2 and dlm MNs with the additional driver lines. **J** Decrease of pulse amplitude upon silencing of hg1, tp1+tp2 and dlm MNs with the additional driver lines. **K** Copulation index of male flies with wing MNs silenced with additional driver lines, after pairing with a virgin female for 15min. **L** Flight ability upon silencing of wing MNs with additional driver lines. Proportion of flies being able to take off and fly for a distance of at least 15 cm (upper graph) and flight ability in a forced flight drop assay (lower graph). **M** Activation of tp2 MN leads to wing lifting. Wing position before activation is shown in green, during activation in magenta. See also video S4. **N** Activation of i2 MN in flight decreases wing beat amplitude, measured by the difference of root mean square values of wing beat oscillograms during 2s before and 2s after onset of activation light. Error bars indicate mean and standard deviation. A-L: Datasets with significant difference to both genetic controls are indicated in blue. * $p < 0.05$, ** $p < 0.005$, *** $p < 0.0005$, **** $p < 0.00005$, Fisher's exact test for box graphs, Kruskal-Wallis test with Dunn's multiple comparison for scatter plots. E-J: only genotypes with significant changes in the indicated song parameter and their respective controls are shown. In scatter plots, error bars indicate median with interquartile range. For song analysis, 20-40 flies of each genotype were tested, and each data point represent one fly in the scatterplots. *TNT*: tetanus toxin. For full genotypes of experimental flies, see Table S2.

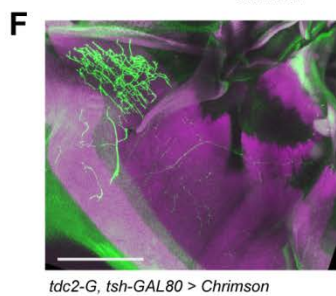
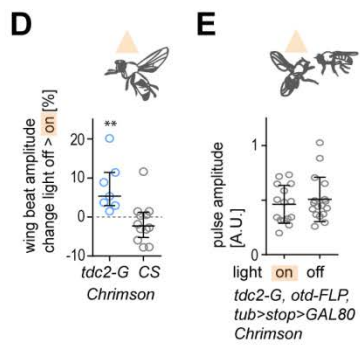
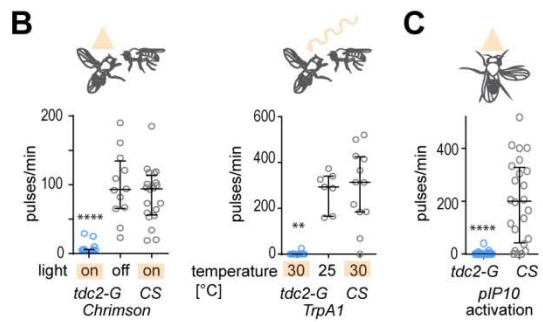
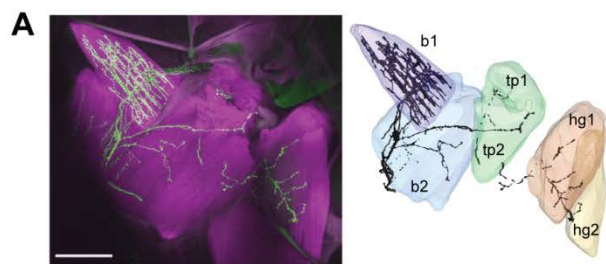


Figure S4. Octopaminergic neurons affect song and flight. Related to Figure 5.

A Octopaminergic neurons (*tdc2-G* driver line) innervate wing muscles (GFP expression in innervations in green, actin phalloidin staining in magenta). Reconstruction of individual steering muscles and the *tdc2* positive axons (black) are shown to the right. **B** Activation of octopaminergic neurons with *Chrimson* (different transgene than shown in Figure 5A) and *TrpA1* during courtship strongly reduces song production. **C** Coactivation of pIP10 and octopaminergic neurons suppresses pIP10 evoked song. **D** Activation of octopaminergic neurons with *Chrimson* (different transgene than shown in Figure 5A) during flight increases wing beat amplitude. **E** Activation of octopaminergic neurons in the VNC and gnathal ganglia during courtship does not change pulse song amplitude. **F** Combining the *tdc2-G* driver line with the *tsh-GAL80* transgene does not remove expression in steering muscle innervations (*Chrimson.Venus* expression in green, actin phalloidin staining in magenta). Scale bars: 100 μ m. B-E: In scatter plots, error bars indicate median with interquartile range, each data point represent one fly. Datasets with significant difference to controls are indicated in blue. * $p < 0.05$, ** $p < 0.005$, *** $p < 0.0005$, **** $p < 0.00005$, Kruskal-Wallis test with Dunn's multiple comparison. For full genotypes of experimental flies, see Table S2.

Table S1 Driver lines used for targeting motor neurons. Related to Figure 3 and 4

abbreviated genotype	full genotype	used in
<i>b2-SG</i>	<i>VT040232.p65ADZp.attp40; VT023830.ZpGAL4DBD.attp2</i>	Figure 3, 4
<i>i2-G</i>	<i>GMR42H07.GAL4.attp2</i>	Figure 3, 4
<i>hg1-SG1</i>	<i>VT010054.p65ADZp.attp40; VT047316.ZpGAL4DBD.attp2</i>	Figure 3, 4
<i>hg1-SG2</i>	<i>VT019911.p65ADZp.attp40; VT010054.ZpGAL4DBD.attp2</i>	Figure S2, S3
<i>hg2-SG1</i>	<i>VT019911.p65ADZp.attp40; VT022025.ZpGAL4DBD.attp2</i>	Figure 3, S3
<i>hg2-SG2</i>	<i>VT022025.p65ADZp.attp2/ VT019911.ZpGAL4DBD.attp2</i>	Figure 4, S2, S3
<i>ps1-SG</i>	<i>VT045969.p65ADZp.attp40; VT045663.ZpGAL4DBD.attp2</i>	Figure 3, 4
<i>tp1-SG</i>	<i>VT022025.p65ADZp.attp2/ VT029310.ZpGAL4DBD.attp2</i>	Figure 3, 4
<i>tp2-SG1</i>	<i>VT045969.p65ADZp.attp40; VT042475.ZpGAL4DBD.attp2</i>	Figure 3, 4
<i>tp2-SG2</i>	<i>VT040232p65ADZp.attp40; VT042475.ZpGAL4DBD.attp2</i>	Figure S2, S3
<i>tp1, tp2-SG</i>	<i>VT040232.p65ADZp.attp40; VT029310.ZpGAL4DBD.attp2</i>	Figure 4, S2, S3, video S3, S4
<i>tpn-SG</i>	<i>VT029310.p65ADZp.attp2/ VT042475.ZpGAL4DBD.attp2</i>	Figure 3, 4
<i>tt-G</i>	<i>VT033051.GAL4.attp2</i>	Figure 3, 4
<i>dIm-SG</i>	<i>GMR23H06.p65ADZp.attp40; GMR30A07.ZpGAL4DBD.attp2</i>	Figure 3, 4
<i>dIm-G</i>	<i>VT021842.GAL4.attp2</i>	Figure 3, S2, S3

Table S2 Full genotypes of flies used in experiments, Related to Figure 2, 3, 4 and 5

Data shown in	Type of experiment	abbreviated genotype	full genotype of experimental flies
Figure 2, S1, video S1	Imaging/activation	<i>pIP10 > ReaChR</i>	<i>w-; LexAop-FRT-stopmCherry-FRT-ReaChR.attp5/UAS-GCaMP6f; GMR22H05.GAL4.attP2/VT040556.LexA.attP2, fruFLP</i>
Figure S1	Imaging/activation	<i>P1 > ReaChR</i>	<i>w-; NP2631.GAL4/UAS-GCaMP6m.attp40; GMR22H05.GAL4.attP2, fruFLP/UAS-FRT-stopmCherry-FRT-ReaChR.VK00005</i>
Figure 3A, S2	Anatomy	<i>b2-SG</i>	<i>w-; UAS-mCD8-GFP/VT040232.p65ADZp.attp40; VT023830.ZpGAL4DBD.attp2/+</i>
Figure 3A, S2	Anatomy	<i>i2-G</i>	<i>w-; UAS-mCD8-GFP/+; GMR42H07.GAL4.attp2/+</i>
Figure 3A, S2	Anatomy	<i>hg1-SG1</i>	<i>w-; UAS-mCD8-GFP/VT010054.p65ADZp.attp40; VT047316.ZpGAL4DBD.attp2/+</i>
Figure 3A, S2	Anatomy	<i>hg2-SG1</i>	<i>w-; UAS-mCD8-GFP/VT019911.p65ADZp.attp40; VT022025.ZpGAL4DBD.attp2/+</i>
Figure 3A, S2	Anatomy	<i>ps1-SG</i>	<i>w-; UAS-mCD8-GFP/VT045969.p65ADZp.attp40; VT045663.ZpGAL4DBD.attp2/+</i>
Figure 3A, S2	Anatomy	<i>tp1-SG</i>	<i>w-; UAS-mCD8-GFP/+; VT022025.p65ADZp.attp2/VT029310.ZpGAL4DBD.attp2</i>
Figure 3A, S2	Anatomy	<i>tp2-SG1</i>	<i>w-; UAS-mCD8-GFP/VT045969.p65ADZp.attp40; VT042475.ZpGAL4DBD.attp2/+</i>
Figure 3A, S2	Anatomy	<i>tpn-SG</i>	<i>w-; UAS-mCD8-GFP/+; VT29310.p65ADZp.attp2/VT039478.ZpGAL4DBD.attp2</i>
Figure 3A, S2	Anatomy	<i>tt-G</i>	<i>w-; UAS-mCD8-GFP/+; VT033051.GAL4.attp2/+</i>
Figure 3A, S2	Anatomy	<i>dIm-SG</i>	<i>w-; UAS-mCD8-GFP/GMR23H06.p65ADZp.attp40; GMR30A07.ZpGAL4DBD.attp2/+</i>
Figure 3A, S2	Anatomy	<i>dIm-G</i>	<i>w-; UAS-mCD8-GFP/+; VT021842.GAL4.attp2/+</i>
Figure S2	Anatomy	<i>hg1-SG2</i>	<i>w-; UAS-mCD8-GFP/VT019911.p65ADZp.attp40; VT010054.ZpGAL4DBD.attp2/+</i>
Figure S2	Anatomy	<i>hg2-SG2</i>	<i>w-; UAS-mCD8-GFP/+; VT022025.p65ADZp.attp2/VT019911.ZpGAL4DBD.attp2</i>
Figure S2	Anatomy	<i>tp1,tp2-SG</i>	<i>w-; UAS-mCD8-GFP/VT040232.p65ADZp.attp40; VT029310.ZpGAL4DBD.attp2/+</i>
Figure S2	Anatomy	<i>tp2-SG2</i>	<i>w-; UAS-mCD8-GFP/VT040232p65ADZp.attp40; VT042475.ZpGAL4DBD.attp2/+</i>
Figure 4, S3	Silencing	<i>b2-SG > TNT</i>	<i>+; UAS-TNT, UAS-mCD8-GFP/VT040232.p65ADZp.attp40; VT023830.ZpGAL4DBD.attp2/+</i>
Figure 4, S3	Silencing control	<i>b2-SG > -</i>	<i>+; VT040232.p65ADZp.attp40/+; VT023830.ZpGAL4DBD.attp2/+</i>
Figure 4, S3	Silencing	<i>i2-G > TNT</i>	<i>+; UAS-TNT/+; GMR42H07.GAL4.attp2/+</i>
Figure 4, S3	Silencing control	<i>i2-G > -</i>	<i>+; +/+; GMR42H07.GAL4.attp2/+</i>
Figure 4, S3A	Silencing	<i>hg1-SG1 > TNT</i>	<i>+; UAS-TNT/VT010054.p65ADZp.attp40; VT047316.ZpGAL4DBD.attp2/+</i>
Figure 4, S3	Silencing control	<i>hg1-SG1 > -</i>	<i>+; VT010054.p65ADZp.attp40/+0; VT047316.ZpGAL4DBD.attp2/+</i>
Figure 4, S3A	Silencing	<i>hg2-SG2 > TNT</i>	<i>+; UAS-TNT, UAS-mCD8-GFP/+; VT022025.p65ADZp.attp2/VT019911.ZpGAL4DBD.attp2</i>
Figure 4, S3	Silencing control	<i>hg2-SG2 > -</i>	<i>+; +/+; VT022025.p65ADZp.attp2/VT019911.ZpGAL4DBD.attp2</i>
Figure 4, S3	Silencing	<i>ps1-SG > TNT</i>	<i>+; UAS-TNT/VT045969.p65ADZp.attp40; VT045663.ZpGAL4DBD.attp2/+</i>
Figure 4, S3	Silencing control	<i>ps1-SG > -</i>	<i>+; VT045969.p65ADZp.attp40/+; VT045663.ZpGAL4DBD.attp2/+</i>
Figure 4, S3	Silencing	<i>tp1-SG > TNT</i>	<i>+; UAS-TNT, UAS-mCD8-GFP/+; VT022025.p65ADZp.attp2/VT029310.ZpGAL4DBD.attp2</i>
Figure 4, S3	Silencing control	<i>tp1-SG > -</i>	<i>+; +/+; VT022025.p65ADZp.attp2/VT029310.ZpGAL4DBD.attp2</i>
Figure 4, S3	Silencing	<i>tp2-SG1 > TNT</i>	<i>+; UAS-TNT/VT045969.p65ADZp.attp40; VT042475.ZpGAL4DBD.attp2/+</i>
Figure 4, S3	Silencing control	<i>tp2-SG1 > -</i>	<i>+; VT045969.p65ADZp.attp40/+; VT042475.ZpGAL4DBD.attp2/+</i>
Figure 4, S3	Silencing	<i>tpn-SG > TNT</i>	<i>+; UAS-TNT, UAS-mCD8-GFP/+; VT029310.p65ADZp.attp2/VT042475.ZpGAL4DBD.attp2</i>
Figure 4, S3	Silencing control	<i>tpn-SG > -</i>	<i>+; +/+; VT029310.p65ADZp.attp2/VT042475.ZpGAL4DBD.attp2</i>
Figure 4, S3	Silencing	<i>tt-G > TNT</i>	<i>+; UAS-TNT/+; VT033051.GAL4.attp2/+</i>
Figure 4, S3	Silencing control	<i>tt-G > -</i>	<i>+; +/+; VT033051.GAL4.attp2/+</i>
Figure 4, S3	Silencing	<i>dIm-SG > TNT</i>	<i>+; UAS-TNT/GMR23H06.p65ADZp.attp40; GMR30A07.ZpGAL4DBD.attp2/+</i>
Figure 4, S3	Silencing control	<i>dIm-SG > -</i>	<i>+; GMR23H06.p65ADZp.attp40/+; GMR30A07.ZpGAL4DBD.attp2/+</i>
Figure 4, S3, video S3	Silencing control	<i>CS > TNT</i>	<i>+; UAS-TNT /+; +/+</i>
Figure 4, S3	Silencing control	<i>GFP > TNT</i>	<i>+; UAS-TNT, UAS-mCD8-GFP/+; +/+</i>
Figure 4C, S3, video S3	Silencing	<i>tp1,tp2-SG > TNT</i>	<i>+; UAS-TNT/VT040232.p65ADZp.attp40; VT029310.ZpGAL4DBD.attp2/+</i>
Figure S3	Silencing	<i>hg1-SG2 > TNT</i>	<i>+; UAS-TNT/VT019911.p65ADZp.attp40; VT010054.ZpGAL4DBD.attp2/+</i>
Figure S3	Silencing control	<i>hg1-SG2 > -</i>	<i>+; VT019911.p65ADZp.attp40/+; VT010054.ZpGAL4DBD.attp2/+</i>
Figure S3	Silencing	<i>tp2-SG2 > TNT</i>	<i>+; UAS-TNT/VT040232p65ADZp.attp40; VT042475.ZpGAL4DBD.attp2/+</i>
Figure S3	Silencing control	<i>tp2-SG2 > -</i>	<i>+; VT040232p65ADZp.attp40/+; VT042475.ZpGAL4DBD.attp2/+</i>
Figure S3	Silencing control	<i>tp1,tp2-SG > -</i>	<i>+; VT040232.p65ADZp.attp40/+; VT029310.ZpGAL4DBD.attp2/+</i>
Figure S3	Silencing	<i>dIm-G > TNT</i>	<i>w-; UAS-TNT/+; VT021842.GAL4.attp2/+</i>
Figure S3	Silencing control	<i>dIm-G > -</i>	<i>w-; VT021842.GAL4.attp2; +/+</i>

Table S2 Full genotypes of flies used in experiments- continued

Data shown in	Type of experiment	abbreviated genotype	full genotype of experimental flies
Figure S3, video S4	Activation	<i>tp1, tp2-SG > Chromson</i>	<i>UAS-CsChrimson.mVenus.attp18; VT040232.p65ADZp.attp40/+; VT029310.ZpGAL4DBD.attp2/+</i>
Figure S3	Activation	<i>i2-G > Chromson</i>	<i>UAS-CsChrimson.mVenus.attp18; +/-; GMR42H07.GAL4.attp2/+</i>
Figure S3	Activation control	<i>i2-G</i>	<i>+; +/-; GMR42H07.GAL4.attp2/+</i>
Figure 5A	Activation	<i>tdc2-G > Chromson</i>	<i>w-; tdc2-Gal4/+; UAS-CsChrimson.mVenus.attp2/+</i>
Figure 5, S4E	Activation VNC, Anatomy	<i>tdc2-G, otd-FLP, tub>stop>GAL80 > Chromson</i>	<i>w-; tdc2-Gal4/Otd-nlsFLPo.attp40; tubP-FRT-stop-FRT-GAL80/UAS-CsChrimson.mVenus.attp2</i>
Figure 5A	Activation	<i>tdc2-G, tub>stop>GAL80 > Chromson</i>	<i>w-; tdc2-Gal4/+; tubP-FRT-stop-FRT-GAL80/UAS-CsChrimson.mVenus.attp2</i>
Figure 5, S4F	Activation brain, Anatomy	<i>tdc2-G, tsh-GAL80 > Chromson</i>	<i>w-; tdc2-Gal4/Tsh-GAL80; UAS-CsChrimson.mVenus.attp2/+</i>
Figure 5A	Activation control	<i>CS > Chromson</i>	<i>w-; +/-; UAS-CsChrimson.mVenus.attp2/+</i>
Figure S4A	Anatomy		<i>w-; UAS-mCD8-GFP/tdc2-Gal4/+; +/-</i>
Figure S4B, D	Activation	<i>tdc2-G > Chromson</i>	<i>UAS-CsChrimson.mVenus.attp18; tdc2-Gal4/+; +/-</i>
Figure S4B, D	Activation control	<i>CS > Chromson</i>	<i>UAS-CsChrimson.mVenus.attp18; +/-; +/-</i>
Figure S4B	Activation	<i>tdc2-G > TrpA1</i>	<i>w-; tdc2-Gal4/UAS-dTrpA1; +/-</i>
Figure S4B	Activation control	<i>CS > TrpA1</i>	<i>w-; UAS-dTrpA1/+; +/-</i>
Figure S4C	Coactivation	<i>plP10, tdc2-G activation</i>	<i>w-; tdc2-Gal4/ UAS-CsChrimson.mVenus.attp40; LexAop-FRT-stopmCherry-FRT-ReaChR.VK00005/VT040556.LexA.attP2, fruFLP</i>
Figure S4C	Coactivation control	<i>plP10, CS activation</i>	<i>w-; tdc2-Gal4/+; LexAop-FRT-stopmCherry-FRT-ReaChR.VK00005/VT040556.LexA.attP2, fruFLP</i>